Expression of Insulin-Like Growth Factor 2 Receptor in Corneal Keratocytes During Differentiation and in Response to Wound Healing

Richard N. Bohnsack,[1] Debra J. Warejcka,[1] Lingyan Wang,[2] Stephanie R. Gillespie,[2] Audrey M. Bernstein,[2] Sally S. Twining,[1,3] and Nancy M. Dahms[1]

[1]Department of Biochemistry, Medical College of Wisconsin, Milwaukee, Wisconsin, United States
[2]Icahn School of Medicine at Mount Sinai, New York, New York, United States
[3]Department of Ophthalmology, Medical College of Wisconsin, Milwaukee, Wisconsin, United States

Correspondence: Nancy M. Dahms, Department of Biochemistry, Medical College of Wisconsin, 8701 Watertown Plank Road, Milwaukee, WI 53226, USA; ndahms@mcw.edu.
Sally S. Twining, Department of Biochemistry, Medical College of Wisconsin, 8701 Watertown Plank Road, Milwaukee, WI 53226, USA; stwining@mcw.edu.

Submitted: July 7, 2014
Accepted: October 11, 2014

Citation: Bohnsack RN, Warejcka DJ, Wang L, et al. Expression of insulin-like growth factor 2 receptor in corneal keratocytes during differentiation and in response to wound healing. *Invest Ophthalmol Vis Sci*. 2014;55:7697–7708. DOI:10.1167/iovs.14-15179

Purpose. Insulin-like growth factor 2 receptor (IGF2R) associates with ligands that influence wound healing outcomes. However, the expression pattern of IGF2R and its role in the cornea is unknown.

Methods. Human keratocytes were isolated from donor corneas. Fibroblasts (fibroblast growth factor 2 [FGF2]–treated) or myofibroblasts (TGF-β1–treated) were analyzed for IGF2R and α-smooth muscle actin (α-SMA) expression by Western blotting and immunolocalization. Mouse corneas were wounded in vivo and porcine corneas ex vivo. The IGF2R and α-SMA protein expression were visualized and quantified by immunohistochemistry. The IGF2R gene expression in human corneal fibroblasts was knocked-down with targeted lentiviral shRNA.

Results. The IGF2R is expressed in epithelial and stromal cells of normal human, mouse, and porcine corneas. The IGF2R increases (11.2 ± 0.4–fold) in the epithelial and (11.7 ± 0.9–fold) stromal layers of in vivo wounded mouse corneas. Double-staining with α-SMA– and IGF2R-specific antibodies reveals that IGF2R protein expression is increased in stromal myofibroblasts in the wounded cornea relative to keratocytes in the normal cornea (11.2 ± 0.8–fold). Human primary stromal keratocytes incubated with FGF2 or TGF-β1 in vitro demonstrate increased expression (2.0 ± 0.4–fold) of IGF2R in myofibroblasts relative to fibroblasts. Conversion of IGF2R shRNA-lentiviral particle transduced corneal fibroblasts to myofibroblasts reveals a dependence on IGF2R expression, as only 40% ± 10% of cells transduced converted to myofibroblasts compared to 86% ± 3% in control cells.

Conclusions. The IGF2R protein expression is increased during corneal wound healing and IGF2R regulates human corneal fibroblast to myofibroblast differentiation.

Keywords: cornea, wound healing, myofibroblasts, IGF2R, TGF-β1

The avascular, transparent cornea provides a protective barrier to the eye and is the major refractive element of the visual system, providing two-thirds of the refractive power of the eye (reviewed previously[1,2]). The cornea is comprised of three major cell-containing layers: an outer stratified epithelium, an extracellular matrix (ECM)–rich stroma layer which constitutes approximately 90% of the thickness of the human cornea, and an endothelium monolayer. The stroma is composed of ECM, with quiescent keratocytes interspersed that synthesize collagens and other ECM molecules.[3]

Wound healing is a complex process involving inflammation, cell migration, differentiation, proliferation, ECM deposition, and ECM remodeling via the action of proteases, such as urokinase-type plasminogen activator (uPA), plasmin, and matrix metalloproteinases (MMPs).[1,4] Corneal wound healing occurs in several distinct, but overlapping, phases: (1) epithelial cells beyond the wound migrate to cover the wound surface, (2) stromal keratocytes near the wound undergo apoptosis, (3) keratocytes surrounding the apoptotic area differentiate to fibroblasts, and along with inflammatory cells migrate into the wound and secrete proteases, components of the ECM, chemokines and growth factors,[5] (4) keratocyte-derived and bone marrow-derived fibroblasts stimulated by TGF-β1 differentiate into myofibroblasts that secrete ECM components and also remodel the ECM,[6–9] and (5) after wound repair, myofibroblasts are removed.[10] Aberrant wound healing due to excessive repair results in fibrosis, a condition observed in numerous tissues, including the cornea, lens, liver, kidney, and lung. Fibrosis is associated with an abundance/persistence of myofibroblasts that contribute to disease progression by overproduction of abnormal ECM, which is deposited in a nonorganized manner, and by excessive contraction.[11,12] Furthermore, corneal haze and scarring results from excessive numbers of myofibroblasts within the stroma layer that aberrantly deposit various components of the ECM.[6,13]

Several molecules that are involved in wound healing interact with the insulin-like growth factor-2 receptor (IGF2R), a 300 kDa multifunctional receptor containing 15 distinct domains (Fig. 1) that specifically binds a diverse set of intracellular and extracellular ligands with high affinity (see reviews[14,15]). These domains mediate the major known functions of the receptor: transporting newly synthesized

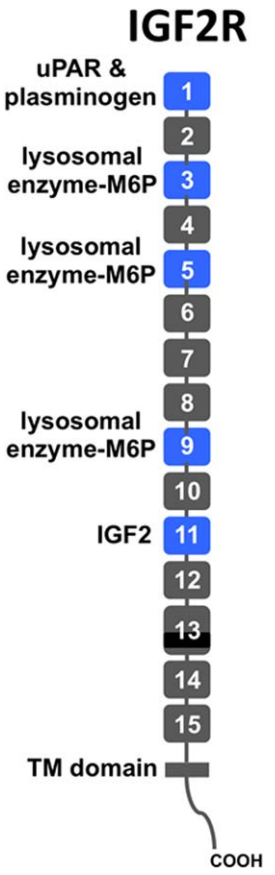

Figure 1. Schematic diagram of IGF2R protein. The IGF2R protein is a type I integral membrane protein with a single transmembrane (TM) domain. It contains 15 contiguous domains (*gray* and *blue rectangles*) in its extracellular region. Each domain is approximately 150 residues in length, except domain 13 is larger and contains a 48-residue fibronectin type II (FnII) insert (*black*). The domains are joined together by a short linker of 5 to 12 residues in length whereas the 15th domain is joined to the transmembrane region by a 25-residue linker. The locations of known ligand binding sites are shown (*blue rectangles*).

lysosomal enzymes from the trans Golgi network to lysosomes; controlling extracellular levels of specific proteins through binding, internalization, and delivery of proteins from the extracellular milieu to lysosomes for degradation; and serving as a scaffold for proteins to interact at the plasma membrane surface. During development, the most important molecule that interacts with the receptor is IGF2, which binds to domain 11 and is delivered to the lysosome for degradation.[16,17] By regulating the circulating levels of IGF2, a growth-promoting polypeptide that signals via the IGF1 and insulin receptors,[18] IGF2R has a critical role in normal development. This key function of the receptor is supported by transgenic mice studies in which the loss of IGF2R results in death at birth, with the embryos displaying an overgrowth phenotype,[19] a phenotype that can be prevented by also knocking down IGF2.[20] In addition, knockdown (KD) of IGF2R in multiple cell types in culture results in mistargeting of lysosomal enzymes to the extracellular milieu and compromised lysosomal function.[21–24] Lysosomal enzymes and other proteins, such as renin precursor and leukemia inhibitory factor, that contain mannose 6-phosphate (M6P) as part of their N-linked high mannose-type glycans, bind to the receptor through domains 3, 5, and 9 (Fig. 1). In addition to lysosomal enzymes and IGF2, IGF2R binds to other key regulators of corneal wound healing, including the urokinase plasminogen activator receptor (uPAR),[25] plasminogen,[26,27] connective tissue growth factor (CTGF),[28] retinoic acid,[29] and heparanase,[30] through mechanisms yet to be elucidated. This receptor may serve as a scaffold for efficient activation of plasminogen by urokinase bound to uPAR through interaction of uPAR and plasminogen to domain 1 (Fig. 1). Binding of the receptor to a number of known molecules involved in corneal wound healing suggests IGF2R also is involved in this process.

The IGF2R is present in most tissues analyzed and its levels are developmentally regulated.[31,32] Microarray analyses of the whole rat cornea 3 and 7 days after excimer laser photorefractive keratectomy (PRK) identified *IGF2R* as one of nine genes increased at the transcript level.[33] No information is available concerning IGF2R protein expression with respect to the various cell types in the cornea. Furthermore, the ligand, IGF2, is present in aqueous humor[34] and in stromal extracts,[35] and IGF2 stimulates the proliferation of keratocytes in culture.[35] Therefore, this study was performed to define the expression pattern of the IGF2R protein in the cornea and to determine whether IGF2R is required for corneal wound healing. The IGF2R was examined in vivo, ex vivo, and in vitro under normal conditions and in response to injury. In addition, a KD strategy was used to evaluate the role of IGF2R in corneal fibroblast differentiation to myofibroblasts.

Materials and Methods

Human Corneal Tissue and Cell Culture Conditions

Human corneas from deidentified organ donors were obtained from the Wisconsin Lions Eye Bank (Madison, WI, USA) within 48 hours of death. Our studies were conducted in compliance with the tenets of the Declaration of Helsinki. The use of deidentified tissue from nonliving individuals is not human subject research as described under section 45 CFR part 46 of the USA Code of Federal Regulations, and this exemption was recognized in writing by the Institutional Review Board.

All experiments were carried out using cells or tissue sections from at least four different donors. Human corneas for immunolocalization were fixed in formalin and embedded in paraffin. The epithelial and endothelial layers of other corneas were scraped from the stroma and the stromal cells were released by collagenase. Proteins were extracted from the cells of the three layers using lysis buffer (50 mM Tris, pH 7.4, 150 mM NaCl, 1% Triton X-100, 0.1% deoxycholate) containing protease inhibitors (Roche Diagnostic Corp., Indianapolis, IN, USA). Total protein was determined by the Bradford method.[36] Primary human corneal epithelial cells were isolated from corneas using Dispase (25 caseinolytic units/ml; Life Technologies, Grand Island, NY, USA). Cells were cultured in defined keratinocyte serum-free medium (Life Technologies). Proteins were extracted from the cells as described above.

Human corneal stromal cells were cultured following removal of endothelial and epithelial layers from the donor corneas, and the stromal cells were released by collagenase digestion as described previously.[37] The cultured fibroblast-like stromal cells were maintained in high glucose Dulbecco's modified Eagle's media (DMEM; Life Technologies) supplemented with 1% L-glutamine (Life Technologies) and 10% fetal bovine serum (FBS; Sigma-Aldrich Corp., St. Louis, MO, USA) at 37°C in a 5% CO_2 atmosphere. Defined phenotypes characteristic of fibroblasts and myofibroblasts were generated by seeding the stromal cells onto collagen (Advanced BioMatrix, San Diego, CA, USA)-coated wells in Defined medium (DMEM plus 1% RPMI vitamin mix; Life Technologies), 100 μM nonessential amino acids, 1 mM pyruvate, 100 μg/mL ascorbic

acid), grown to confluence, and then treated for seven days by adding either 10 ng/mL fibroblast growth factor 2 (FGF2, promotes fibroblast phenotype; Life Technologies) or 1 ng/mL TGF-β1 (promotes myofibroblast phenotype; R & D Systems, Minneapolis, MN, USA) to the Defined medium.[38]

Murine Corneal Tissue

Our studies with mice adhered to the Association for Research in Vision and Ophthalmology (ARVO) Statement for the Use of Animals in Ophthalmic and Vision Research. This study was done in strict accordance with the recommendations in the Guide for the Care and Use of Laboratory Animals. The protocol was approved by the Institutional Animal Care and Use Committee (IACUC, AUA00002232), and buprenorphine was administered subcutaneously to minimize pain. The C57Bl6/J mice were anesthetized with isoflurane, and proparacaine drops were instilled in the experimental eye. A trephine was used to outline a 2-mm circle on the cornea. To generate an epithelial scrape injury, the epithelial layer was removed within the outlined area using an Alger brush. After 7 days, the mice were euthanized, and the eyes were removed and fixed in 10% phosphate-buffered formalin.

Immunohistochemistry of Human and Murine Corneas

Formalin-fixed, paraffin-embedded human or murine corneal sections were deparaffinized, rehydrated, and treated with 10 mM citrate buffer containing 0.05% Tween 20 at pH 6 at 100°C for 10 minutes for antigen retrieval. After blocking, sections were incubated with IGF2R-specific antibodies (for human corneal sections, 1:200 dilution of product #PA3-850 polyclonal rabbit serum [ThermoFisher, Waltham, MA, USA] was used or for murine corneal sections, 1:200 dilution of B14.5 polyclonal rabbit serum[23,39]) or the corresponding preimmune serum at 4°C overnight. Biotinylated secondary antibody, VECTASTAIN ABC-avidin alkaline phosphatase reagent, and Vector Red alkaline phosphatase fluorescent substrate (Vector Laboratories, Burlingame, CA, USA) were used for detection of the primary antibody. Sections were examined using a Nikon Eclipse 80i microscope equipped with a Nikon DS-Fi1 camera and Elements D software (Nikon, Melville, NY, USA) for image capture. The Texas Red excitation and emission filters were used. Images were quantified using auto measure plus module of axiovision 4.8.1 software (Zeiss, Jena, Germany). The morphometric analysis was setup on a positive control slide using the pixel intensity of alkaline phosphatase stain to segment positively stained areas (thresholding); preimmune serum staining was used to set the threshold pixel intensity. The software also generates a postprocessed image of the segmented area for each image; thus, providing visual confirmation. For quantifying positive staining in either epithelial or stromal region, the data were corrected by manual removal method of the epithelial or stromal area. The percent stained area was calculated by measurement of the total alkaline phosphatase positive area above the threshold/total epithelium or stroma image area in square microns.

Porcine Corneal Organ Culture, Immunohistochemistry, and Immunofluorescence Staining

Porcine eyes purchased from Pel-Freez (Rogers, AR, USA) were sterilized with iodine before performing a 5-mm anterior keratectomy. In this model, corneas are wounded by anterior keratectomy using a sharp-edged cylinder to create a wound through the epithelium, basement membrane, and the anterior stroma with subsequent removal of the incised tissue. Untreated or wounded corneas were removed with 2-mm scleral rims, mounted on an agar base containing 1% agarose and 1 mg/mL bovine collagen (Purcol; Advanced Biomatrix, Poway, CA, USA). The DMEM-F12 medium (Life Technologies) containing gentamycin and α-D-glucopyranosyl ascorbic acid was added to cover the sclera to the level of the limbus, and the air-exposed epithelium was moistened daily and the culture medium was changed every other day for 2 weeks as described.[40] After 2 weeks, the corneas were fixed in formalin and paraffin embedded. Deparaffinized sections were incubated in 10 mM citrate buffer pH 6.4 at 100°C for 5 minutes for antigen retrieval. Following blocking for nonspecific binding, sections were prepared for either 3,3′-diaminobenzidine (DAB) and hematoxylin staining using horseradish peroxidase (HRP)–conjugated goat anti-rabbit antibody and DAB peroxidase substrate kit (Vector Laboratories) or immunofluorescence imaging (triple-labeled with antibodies specific for IGF2R (1:200 dilution of ThermoFisher product #PA3-850 and Alexa Fluor 488 Goat Anti-Rabbit IgG [Life Technologies] as the secondary antibody) and α-smooth muscle actin (α-SMA, Cy5 conjugated; Sigma-Aldrich Corp.), with nuclei stained with DAPI. Fluorescence microscopy was carried out using a Zeiss Axioplan2 microscope at the Microscopy Shared Resource Facility at the Icahn School of Medicine at Mount Sinai with the filter sets ET 470/40x and ET525/50m for Alexa Fluor 488, and ET 620 and ET700/75m for Cy5. Using ImageJ (National Institutes of Health [NIH], Bethesda, MD, USA) threshold pixel intensity was set for all images, and the area in the stroma greater than the threshold measurement was quantified for each image. Values are reported as the mean ± SE.

Immunocytochemistry of Cultured Human Cells

Cultured human corneal fibroblasts and myofibroblasts were washed with PBS and fixed for 20 minutes on ice with 10% (vol/vol) formalin in PBS. After fixing, cells were incubated in PBS containing 0.1% Triton X-100 (vol/vol) for 5 minutes at room temperature. Fluorescein-conjugated antibody specific to α-SMA (Sigma-Aldrich Corp.) was diluted 1:100 in PBS containing 10 mg/mL BSA and 0.01 μg/mL Hoechst H33342 stain (Life Technologies) and incubated overnight at 4°C. The cells were washed with PBS and imaged on a Nikon Eclipse Ti fluorescent microscope equipped with a Nikon Digital Sight DS-Qi1MC camera using NIS Elements D3.10.Ink software package. The LAMP1 staining was done as above using a 1:200 dilution of the monoclonal antibody H4A3 developed by J. T. August and J. E. K. Hildreth (Developmental Studies Hybridoma Bank, University of Iowa, Iowa City, IA, USA, under the auspices of the National Institute of Child Health and Human Development, NIH) and a 1:1000 dilution of goat anti-mouse antibody conjugated to Alexa Fluor 568 (Life Technologies). The IGF2R was detected using IGF2R-specific antibody at a 1:100 dilution (ThermoFisher product #PA3-850) in PBS containing 0.1% BSA and 0.1% saponin and a 1:1000 dilution of chicken anti-rabbit antibody conjugated to Alexa Fluor 594 (Life Technologies). Double-staining for the detection of F-actin and α-SMA was conducted using 1:200 dilution of fluorescein-conjugated phalloidin (Sigma-Aldrich Corp.) and 1:200 dilution of α-SMA–specific antibody (Abcam, Cambridge, MA, USA) with a 1:500 dilution of goat anti-mouse antibody conjugated to Alexa Fluor 568 (Life Technologies), respectively. To compare expression levels between the fibroblast and myofibroblast phenotype for each of the above proteins, the same exposure time was used when imaging the stained cells. Negative controls without a primary antibody were included in each experiment as well as using the corresponding preimmune

Investigative Ophthalmology & Visual Science

serum for the IGF2R-specific antibody. Cells were identified as myofibroblasts by analyzing approximately 200 to 500 cells per micrograph for the presence of assembled α-SMA fibrils.

Western Blot Analyses

The proteins from the dissected human corneal layers were extracted as described above and loaded onto SDS-PAGE gels in Laemmli SDS-PAGE sample buffer based on protein content. Cultured human stromal fibroblast and myofibroblast lysates were generated in Laemmli SDS-PAGE sample buffer and an equivalent number of cells (fibroblasts or myofibroblasts) were loaded into each lane of SDS-PAGE gels. The number of cells was determined by counting Hoechst H33342 (Life Technologies) stained nuclei using ImageJ software (version 1.46r; NIH). Nuclei were imaged using a Nikon Eclipse Ti fluorescent microscope and four random images were taken for each well. Proteins were transferred electrophoretically to Immobilon-P PVDF membrane (ThermoFisher) and subjected to quantitative Western blot analyses as described previously.[39] Briefly, after incubating the membranes with antibodies specific to IGF2R (product #PA3-850; ThermoFisher), α-SMA (Abcam), or LAMP1 (Cell Signaling Technology, Inc., Danvers, MA, USA), the membranes were probed with horseradish peroxidase-conjugated Protein A (ThermoFisher) or goat anti-mouse IgG (ThermoFisher). The proteins were visualized using SuperSignal WestPico enhanced chemiluminescence reagents (ThermoFisher), and the resulting bands were quantified using a Bio-Rad ChemiDoc XRS+ system and Image Lab software (Bio-Rad Laboratories, Inc., Hercules, CA, USA).

Relative Quantitative Real-Time PCR

Total RNA was extracted from cultured human corneal stromal fibroblasts and myofibroblasts derived from four human cornea donors using the RNeasy kit (Qiagen, Valencia, CA, USA) and the amount of RNA isolated was quantified by optical density at 260 nm. RNA (1 μg) from each sample was reverse transcribed to cDNA using SuperScript III First-Strand Synthesis System (Life Technologies). Real-time PCR amplification of IGF2R cDNA was performed with previously published primers (forward primer, 5′-GAGGGAAGAGGCAGGAAAG-3′ and reverse primer, 5′-TGTGGCAGGCATACTCAG-3′)[41] using Bullseye EvaGreen qPCR Master Mix (MidSci, St. Louis, MO, USA) with 6′carboxyl-X-Rhodamine (ROX) as the reference dye in an Applied Biosystems 7500 System (Life Technologies). The results of real-time PCR were analyzed by the comparative threshold cycle method and normalized to glyceraldehyde 3-phosphate dehydrogenase (GAPDH; forward primer, 5′-TCGAC AGTCAGCCGCATCTTCTTT-3′ and reverse primer, 5′-ACC AAATCGGTTGACTCCGACCTT-3′) as an internal control. The relative quantity of IGF2R was compared to the relative quantity of GAPDH for every sample. Each sample was run in triplicate. The DNA sequencing of each sample confirmed the identity of the amplified PCR product as IGF2R.

Lentivirus-Mediated KD of IGF2R

Knockdown of IGF2R expression was performed in primary human keratocytes using lentivirus to deliver short hairpin RNA interference (shRNAi). Lentiviral delivery of a shRNA expression cassette specific for the human IGF2R was performed using the sequence 5′-GCCCAACGATCAGCACTT CttcaagagaGAAGTGCTGATCGTTGGGC-3′, a shRNA previously shown to efficiently reduce IGF2R protein expression in human cancer cells.[24] The shRNA sequence was cloned into the AgeI and EcoRI sites of the Addgene pLKO.1hygro plasmid 24150, which encodes a hygromycin resistence gene for selection (developed by R. Weinberg and obtained from Addgene, Cambridge, MA, USA) to make pLKOhygro6588. The insert was confirmed by DNA sequencing. Virus particles were produce by cotransfecting HEK293T cells with pLKOhygro6588 or pLKO.1hygro plasmid and helper plasmids using TransIT-293 transfection reagent (Mirus Bio LLC, Madison, WI, USA) according to the manufacturer's protocol. Briefly, HEK293T cells were plated at 2×10^5 cells/well on 6-well plates 24 hours before transfection. The pLKOhygro6588 or pLKO.1hygro plasmid and helper plasmids were incubated with the TransIT-293 reagent in Opti-MEM serum-free medium (Life Technologies) at room temperature for 30 minutes before addition to HEK293T cells. After 18 hours, the medium containing the transfection reagents was removed from the HEK293T cells and replaced with DMEM medium supplemented with 10% FBS and 1.1% BSA (viral collection medium). Following incubation for 24 hours, the medium was replaced with fresh viral collection medium and the cells were incubated an additional 24 hours. The viral particles were concentrated from the medium by centrifugation at 17,500*g* for 3 hours at 4°C and resuspended in 0.1 times the original volume of DMEM, 10% FBS with 8 mg/mL polybrene (Sigma-Aldrich Corp.) yielding a ×10 concentrated stock of viral particles. Transduction of human corneal fibroblasts to decrease IGF2R protein expression was conducted with freshly prepared viral particles. Briefly, primary corneal cells were plated at 4×10^5 cells/well on 6-well plates 24 hours before infection. Cells were washed with PBS and incubated with 1 mL of the concentrated viral particles. After 3 hours, 1 mL of DMEM medium was added and the cells were incubated for 18 hours. After 18 hours, the viral particle-containing medium was replaced with DMEM containing 10% FBS.

Statistics

Statistical analyses were performed using Sigma Plot 12.5 (Systat, San Jose, CA, USA) A 1-tailed Student's *t*-test was performed for comparison of the differences in IGF2R immunostaining in wounded murine and porcine corneas versus nonwounded. This method also was used to compare the levels of mRNA for IGF2R in fibroblasts versus myofibroblasts. The protein levels of IGF2R, LAMP1, and α-SMA in cells treated with TGF-β1 versus FGF2 were compared to a hypothetical ratio of 1.0 using a 1-sample Student's *t*-test. For comparison of the effects of knocking down IGF2R on the levels of IGF2R, Lamp1, and α-SMA, the wild type (WT) cell levels of the proteins was set to 100%, and the KD and pLKO vector control were calculated relative to the WT. The protein values for the IGF2R KD samples were compared to the pLKO vector control using the 1-tailed Student's *t*-test. For comparison of the studies determining the effects of knocking down the *IGF2R* gene on conversion of corneal stromal cells to myofibroblasts, overall differences were determined by a 1-way ANOVA followed by multiple comparisons using the Holm-Sidak method. Data are presented as the mean ± SE.

Results

IGF2R Protein Expression in Corneal Tissue

To evaluate the location of IGF2R within the normal cornea, immunohistochemistry was performed on tissue sections from human, mouse, and pig corneas. The results showed that IGF2R is present in the epithelial and stromal layers of normal, unwounded cornea (Figs. 2A, 3A, 4F). Most of the cells of the human epithelium stained for IGF2R; however, most of the staining for the mouse and porcine corneas was associated

Investigative Ophthalmology & Visual Science

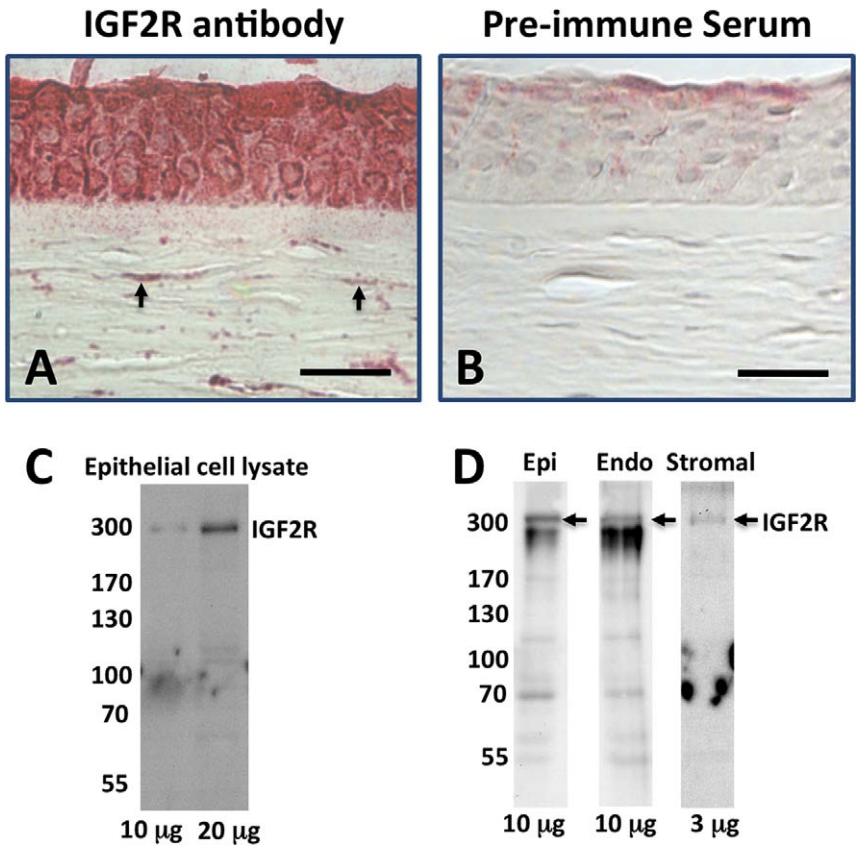

Figure 2. Immunodetection of IGF2R in tissue sections from human cornea. Normal human donor corneas (**A**, **B**), were formalin-fixed, paraffin-embedded, and sections incubated with IGF2R-specific polyclonal antibody (**A**) or the corresponding pre-immune serum (**B**). Biotinylated secondary antibody, avidin alkaline phosphatase reagent and a fluorescent Vector Red alkaline phosphatase substrate were used for detection of the primary antibody. *Scale bar*: 40 µm. *Arrows* indicate representative cells in the stroma with intense staining for IGF2R. (**C**) Cultured primary human epithelial cell lysates were subjected to Western blot analysis and the membranes probed with IGF2R-specific antibody. The amount of total protein from the cell lysate loaded in each lane is indicated. (**D**) Lysates from human corneal epithelial, stromal, and endothelial cell layers were subjected to Western blot analysis and the membranes probed with IGF2R-specific antibody. The amount of total protein from the cell lysate loaded in each lane is indicated. All bands below the 300 kDa IGF2R-labeled bands in (**C**, **D**) are nonspecific and appear in blots using the preimmune serum.

with basal epithelium. In addition, Western blots of cultured primary human epithelial cells, and human corneal epithelial, stromal, and endothelial layer extracts confirmed the presence of IGF2R in all corneal layers (Figs. 2C, 2D).

We then asked if wounding altered IGF2R expression in the cornea in vivo. For these studies involving inflicted wounds we used a standard in vivo mouse epithelial wound model and a porcine organ culture model of corneal wounding, which removed the central epithelial layer and the anterior portion of the stroma. Mouse corneas were subjected to a 2-mm diameter epithelial scrape wound and allowed to heal for 7 days in vivo. Nonspecific preimmune staining of the wounded epithelial layer was much greater than observed for the nonwounded cornea. The IGF2R localization studies demonstrated that wounding the cornea increases IGF2R expression in the central epithelium by 11.2 ± 0.4–fold and stroma by 11.7 ± 0.9–fold (Figs. 3A, 3C, 3E). To confirm this result in another wounding model involving the stroma, the porcine corneal organ culture model was chosen because this model uses a large cornea that undergoes wound healing similar to that observed in the human.[40] The porcine corneas were wounded by removal of a 5-mm trephined central portion of the epithelial, basement membrane, and stroma layers, and allowed to heal for 14 days in organ culture (Fig. 4). Consistent with the in vivo wounded murine cornea, a dramatic increase in IGF2R by 11.2 ± 0.8–fold was observed in the wounded porcine stroma compared to control (Figs. 4A, 4C, 4E). Immunostaining using an Alexa Fluor 488–labeled secondary antibody for IGF2R was increased in the epithelium and stroma of the wounded cornea relative to that of the nonwounded cornea (Figs. 4F, 4G). This is consistent with the results in the murine model of corneal wounding (Figs. 3A, 3C). The epithelial staining for IGF2R was not observed using the colorimetric HRP-diaminobenzidine staining system (Figs. 4A, 4C), which is likely due to decreased sensitivity of this system relative to the Vector Red fluorophore used for the murine system (Figs. 3A, 3C) and the Alexa Fluor 488 fluorophore used for the porcine system (Figs. 4F, 4G).

We next asked if the IGF2R-positive cells in the cornea stromal layer were myofibroblasts. The differentiation of fibroblasts to myofibroblasts can be identified by the expression of α-SMA, and its assembly into stress fibers is an established marker of myofibroblasts in vitro and in vivo.[42–44] Double-staining with α-SMA– and IGF2R-specific antibodies revealed that the dramatic increase in IGF2R expression observed in the stromal layer of the wounded porcine cornea occurs in myofibroblasts (Figs. 4F–K). An increase in the level of α-SMA also was noted in the wounded epithelial layer consistent with the increase in this protein during corneal epithelial-mesenchymal transition (EMT) following wounding.[45,46]

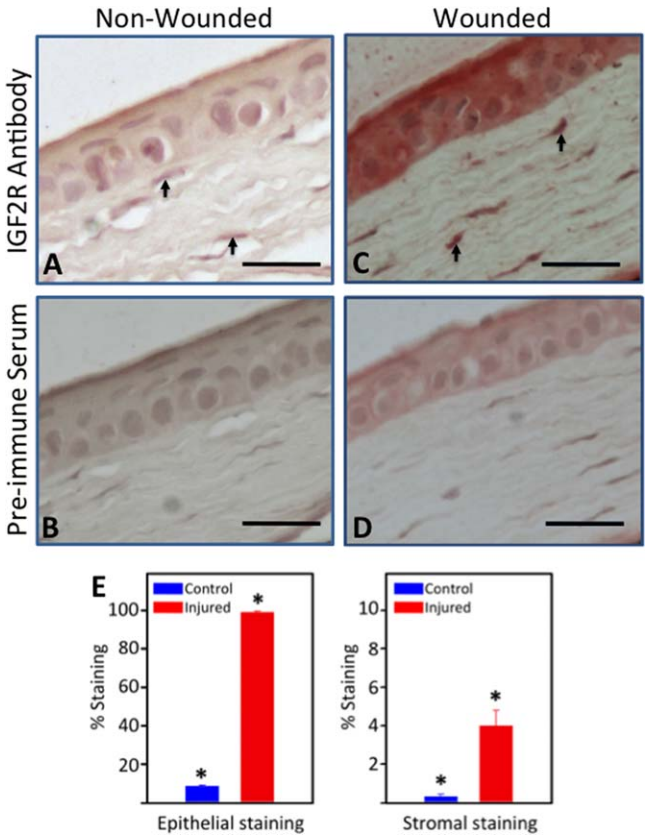

Figure 3. Immunodetection of IGF2R in tissue sections from wounded mouse cornea. Normal mouse corneas (**A**, **B**) or mouse corneas subjected to a 2-mm central scraped wound limited to the epithelial layer (**C**, **D**) were formalin-fixed, paraffin-embedded, and sections incubated with IGF2R-specific polyclonal antibody (**A**, **C**) or the corresponding preimmune serum (**B**, **D**). Biotinylated secondary antibody, avidin alkaline phosphatase reagent, and a fluorescent Vector Red alkaline phosphatase substrate were used for detection of the primary antibody. A representative experiment is shown of three independent replicates. Mouse corneas represent the unwounded central cornea (**A**, **B**) and the center of the wound bed (**C**, **D**). *Scale bar*: 40 μm. *Arrows* indicate representative cells in the stroma with intense staining for IGF2R. (**E**) Quantification of IGF2R staining area in the epithelial and stromal layers of control and wounded mouse samples is shown. Stained areas were above the threshold set based on the preimmune staining. The values represent the mean ± SE. *Indicates 1-tailed Student's *t*-test, $P < 0.005$.

Alteration of IGF2R Expression Levels by TGF-β1–Stimulated Differentiation of Fibroblasts to Myofibroblasts in Culture

During the wound repair process, corneal stromal fibroblasts stimulated at least in part by TGF-β1 differentiate into myofibroblasts,[6–9] a process that can be recapitulated in vitro.[38] To determine whether IGF2R expression changes upon stromal keratocyte differentiation in vitro, primary human corneal serum-cultured keratocytes (fibroblasts) subsequently were cultured on collagen type I–coated wells for 7 days in supplemented serum-free medium containing either FGF2 or TGF-β1 to maintain the fibroblast or promote the myofibroblast phenotype, respectively. The dramatic increase in α-SMA protein (25.8 ± 9.0–fold; Figs. 5A, 5B) and assembled α-SMA stress fibers (Fig. 5D) confirmed the TGF-β1–mediated conversion of fibroblasts to myofibroblasts in vitro. Western blot analyses of the FGF2- and TGF-β1–treated cells demonstrated increased expression (2.0 ± 0.4–fold) of IGF2R in myofibroblasts relative to fibroblasts (Figs. 5A, 5B). These elevated IGF2R protein levels mirrored the 1.8 ± 0.2–fold increase in IGF2R transcript levels observed in myofibroblasts compared to fibroblasts (Fig. 5C). Immunofluorescence microscopy further supports the increased expression of IGF2R upon differentiation of fibroblasts to myofibroblasts (Fig. 5D). Taken together, these in vivo and in vitro results provided the first characterization of IGF2R protein expression in the cornea. Importantly, the results demonstrated upregulation of IGF2R protein during corneal wounding and in the process of fibroblast to myofibroblast differentiation. Furthermore, these results showed that alterations in IGF2R protein levels upon fibroblast to myofibroblast differentiation are mediated primarily by transcriptional regulation of the *IGF2R* gene.

Because one of the many cellular roles of *IGF2R* is delivering newly synthesized lysosomal enzymes to lysosomes, we asked whether the increased expression of *IGF2R* in myofibroblasts represents an expansion of endosomal/lysosomal compartments that may be needed for remodeling of the ECM by myofibroblasts. As an indirect measure of the number of endosomes/lysosomes, we quantified lysosome-associated membrane protein 1 (LAMP1), an established marker of late endosomes and lysosomes.[47] The LAMP1 protein is among the most abundant lysosomal membrane proteins and its extensive glycosylation aids in protecting the luminal membrane of the lysosome from degradation by resident lysosomal hydrolytic enzymes.[48] Western blot analysis demonstrated a 3.3 ± 0.9–fold higher amount of LAMP1 in myofibroblasts compared to fibroblasts (Figs. 5A, 5B). Immunofluorescence microscopy further supported the increased expression of LAMP1 upon differentiation of fibroblasts to myofibroblasts (Fig. 5D). The observed increase in LAMP1 levels is consistent with an expansion of the endosomal/lysosomal system in myofibroblasts compared to fibroblasts.

Requirement of IGF2R for the Conversion of Fibroblasts to Myofibroblasts

To begin to evaluate the role of IGF2R in the cornea, silencing of endogenous IGF2R in human primary corneal fibroblast-like cells was performed with lentiviral-based short hairpin RNA (shRNA) to reduce IGF2R transcript levels. Human corneal stromal cells can be transduced with lentivirus particles,[49] and lentivirus delivery of shRNA is a method to silence gene expression by RNA interference (RNAi) in human corneal cells.[50] Lentiviral delivery of an shRNA expression cassette specific for the human IGF2R was performed using an shRNA previously shown to reduce IGF2R protein expression in human cancer cells.[24] The IGF2R KD experiments using human corneal stromal cells resulted in an approximately 50% reduction of IGF2R protein expression relative to cells transfected with an empty cassette (pLKO) and to WT cells (Fig. 6A).

In contrast to the parallel upregulation of IGF2R and LAMP1 upon TGF-β1–mediated conversion of fibroblasts to myofibroblasts (Figs. 5A, 5B), the levels of the lysosomal protein LAMP1 are not significantly different in the IGF2R KD cells when compared to control cells (Fig. 6A). These results showed that altering IGF2R protein levels do not affect the expression of LAMP1, indicating that TGF-β1–activated signaling pathways, but not IGF2R-mediated pathways, regulate the number of endosomal and/or lysosomal compartments.

We also evaluated the effect of decreased IGF2R levels on α-SMA expression by Western blot analysis. These data demonstrated approximately 25% less compared to cells transduced with the pLKO control vector and approximately 40% less α-

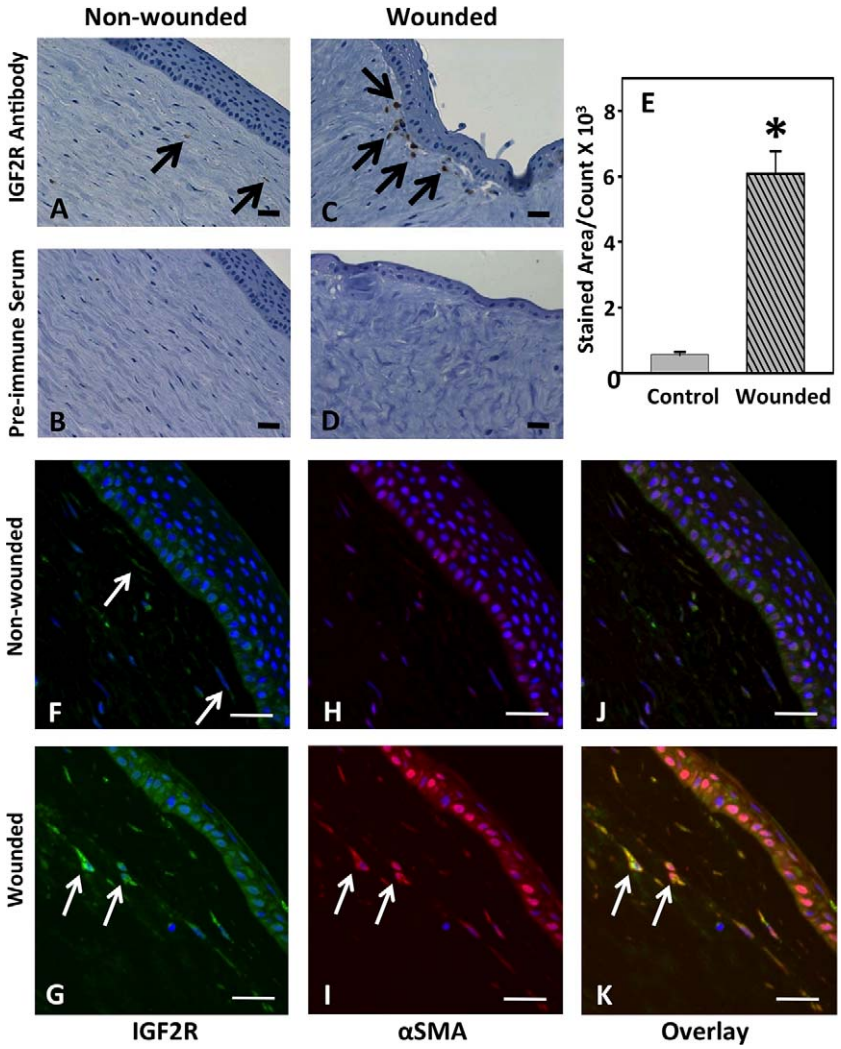

Figure 4. Immunodetection of IGF2R in organ cultures of normal or trephine-wounded porcine corneas. Untreated porcine corneas (**A**, **B**, **F**, **H**, **J**) or those wounded by removal of 5 mm trephined portion of the cornea, including epithelium and the anterior stroma (**C**, **D**, **G**, **I**, **K**), were mounted on a base containing agarose and collagen as described.[40] The corneas were cultured for 2 weeks, fixed, and sections were obtained. (**A**–**D**) Sections were incubated with IGF2R-specific polyclonal antibody (**A**, **C**) or the corresponding preimmune serum (**B**, **D**) followed by HRP-conjugated goat anti-rabbit antibody and colorimetric DAB substrate. Sections were counterstained with hematoxylin. A representative experiment is shown of three independent replicates. *Arrows* in (**C**) indicate regions of the stroma with intense staining for IGF2R. Quantification of IGF2R staining area in the control and wounded samples is shown in (**E**), and the values represent the mean ± SE. A 1-tailed Student's *t*-test, $P < 0.001$. (**F**–**K**) Immunofluorescence imaging was performed by double-labeling with antibodies specific for IGF2R ([**F**, **G**], *green,* Alexa Fluor488) and α-SMA ([**H**, **I**], *red,* Cy5), and nuclei are stained with DAPI (*blue*). Overlay of images is shown in (**J**, **K**). A representative experiment is shown of three independent replicates. *Arrows* in (**G**, **I**, **K**) highlight representative myofibroblasts that stain positive for both IGF2R and α-SMA. *Scale bar*: 100 μm.

SMA in the IGF2R KD cells compared to WT control cells (Fig. 6A). Correspondingly, after 7 days in culture in the presence of TGF-β1, 86% ± 3% of cells transduced with the pLKO control vector lentiviral particles or 87% ± 3% of nontransduced (i.e., WT) cells converted to myofibroblasts as assessed by the presence of α-SMA–containing fibrils, whereas only 40% ± 10% of cells transduced with shRNA-IGF2R lentiviral particles were observed to express α-SMA–containing fibrils (Figs. 6B, 6C). Phalloidin staining shows that this decrease in α-SMA–containing fibrils is not due to a lack of F-actin fibrils in the IGF2R KD cells (Fig. 6B). Together, these results demonstrate IGF2R is required for corneal fibroblast upregulation of α-SMA synthesis, assembly of α-SMA–containing fibrils and differentiation to myofibroblasts.

Discussion

The current report provides the first characterization of IGF2R protein expression in the cornea to our knowledge. The IGF2R protein is localized in corneal stromal and epithelial cells and its level is increased upon corneal injury. In the wounded cornea, a dramatic increase in IGF2R expression in the stromal layer occurs in myofibroblasts. The 2-fold higher IGF2R protein levels in myofibroblasts relative to fibroblasts in vitro correlates directly with the 1.8-fold increase observed in IGF2R transcript levels, indicating that alterations in IGF2R protein levels upon fibroblast to myofibroblast differentiation are due to transcriptional regulation of the *IGF2R* gene. A similar process occurs in the liver; upregulation of IGF2R transcription has been reported in hepatic stellate cells during fibrogenesis.[51] Taken

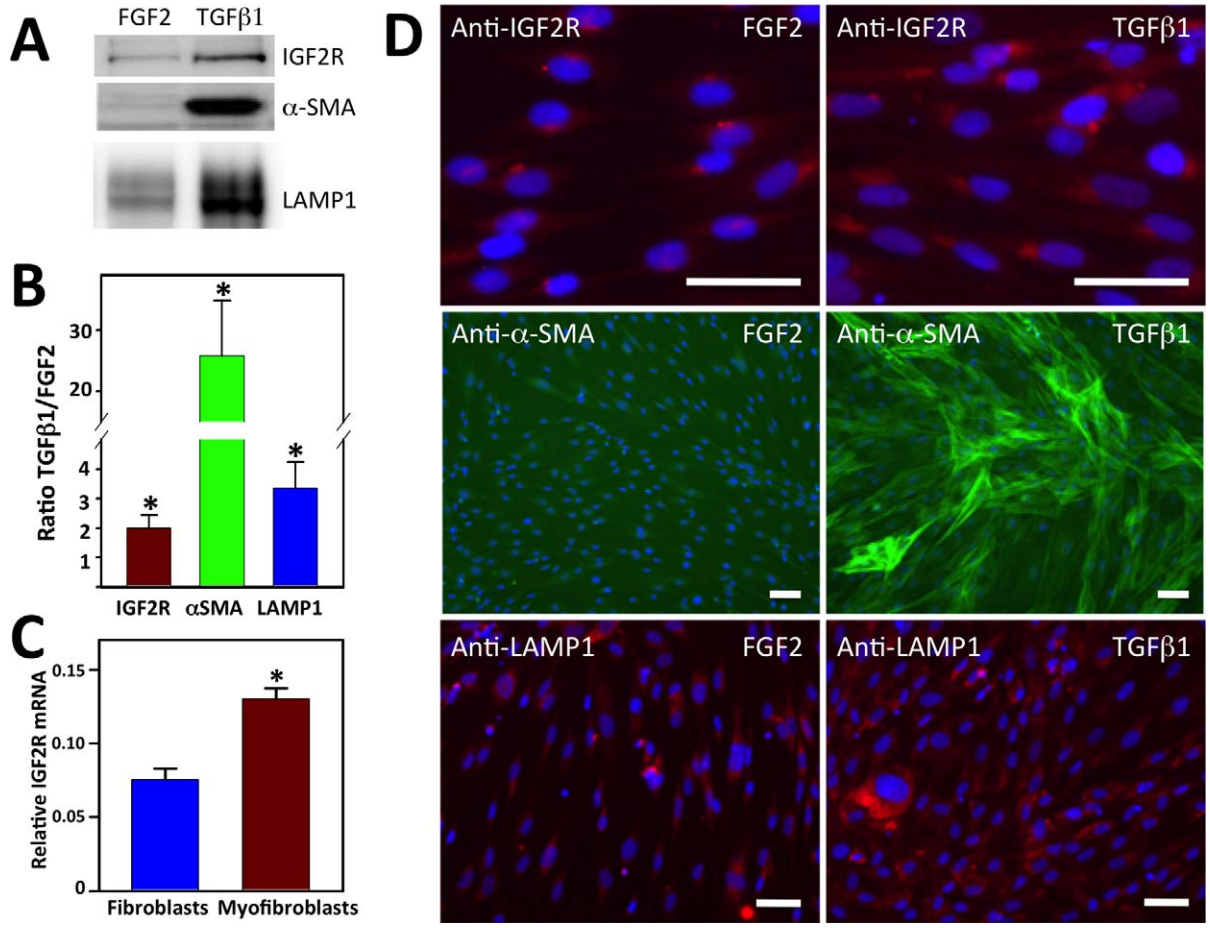

Figure 5. Comparison of IGF2R, α-SMA, and LAMP1 levels in myofibroblasts to fibroblasts. (**A**) Lysates generated from human donor corneal keratocytes cultured in serum-free medium supplemented with 10 ng/mL FGF2 or 1 ng/mL TGF-β1 for 7 days were subjected to Western blot analysis. Extracts of equivalent cell numbers were loaded into each lane. Membranes were probed with antibodies specific to IGF2R, α-SMA, or LAMP1. (**B**) Quantification of (**A**) is shown which represents an analysis of corneal keratocyte lysates obtained from independent donors ($n = 6$, IGF2R; $n = 6$, α-SMA; $n = 5$, LAMP1). Values represent the mean ± SE. A 1-sample Student's *t*-test with a hypothetical population mean = 1.0, $P < 0.05$. (**C**) Real-time PCR analyses of IGF2R mRNA. (**C**) Total RNA obtained from cultured fibroblasts and myofibroblasts derived from four independent human donor corneas was analyzed. The relative quantity of IGF2R was compared to the relative quantity of GAPDH, which was used as an internal control. Replicates were performed in triplicate. Values represent the mean ± SE. Student's *t*-test $P < 0.001$. (**D**) Human donor corneal keratocytes cultured in 10 ng/mL FGF2 or 1 ng/mL TGF-β1 for 7 days were fixed, incubated with IGF2R-specific antibodies and visualized using a chicken anti-rabbit secondary antibody conjugated to Alexa Fluor 594 (*red*), FITC-conjugated antibody specific to α-SMA (*green*), or LAMP1-specific antibodies visualized using a mouse anti-rabbit secondary antibody conjugated to Alexa Fluor 568 (*red*), and then imaged. Nuclei were stained with Hoescht 33342 dye (*blue*). *Scale bar*: 100 μm.

together, the results demonstrated that elevation of IGF2R protein levels occurs as a consequence of corneal wounding and the process of TGF-β1–stimulated differentiation of fibroblasts to myofibroblasts.

Using a KD strategy, this study also shows that IGF2R is required for corneal fibroblast differentiation to myofibroblasts as assessed by assembly of α-SMA into fibrils, which is a characteristic feature of the myofibroblast phenotype.[43] The IGF2R level correlates directly with the ability of α-SMA to assemble into fibrils as only 40% ± 10% of cells transduced with shRNA-IGF2R lentiviral particles converted to myofibroblasts compared to 86% ± 3% in cells transduced with the pLKO control vector lentiviral particles or 87% ± 3% in nontransduced cells. Similar findings were reported by Hao et al.[52] using rat lung fibroblasts. In this study, differentiation of primary rat lung fibroblasts to myofibroblasts was induced by free silica, and the expression level of α-SMA and IGF2R was observed to be higher in myofibroblasts compared to fibroblasts.

These results lead to the question, "What are the possible mechanisms of action by which IGF2R could impact fibroblast to myofibroblast differentiation"? The IGF2R interacts with numerous M6P-containing and non-M6P–containing ligands that influence corneal biology and wound healing. In the in vivo mouse and ex vivo porcine models, IGF2R may be required for activation of latent TGF-β1 complex. This complex is composed of the TGF-β homodimer, the latency-associated peptide and latent TGF-β–binding protein. One proposed mechanism for activation of this complex is through its binding to IGF2R via a M6P-containing N-glycan on the latent-associated peptide.[53] Binding of the latent TGF-β complex to the receptor is thought to facilitate proteolysis by juxtaposing the cleavage site of the latency-associated peptide with IGF2R-bound proteases to release active TGF-β1.[54]

The IGF2R protein must be critical for other mechanisms involved in TGF-β1–induced conversion of fibroblasts to myofibroblasts because in the cell culture studies reported here, active TGF-β1, which does not contain an M6P-

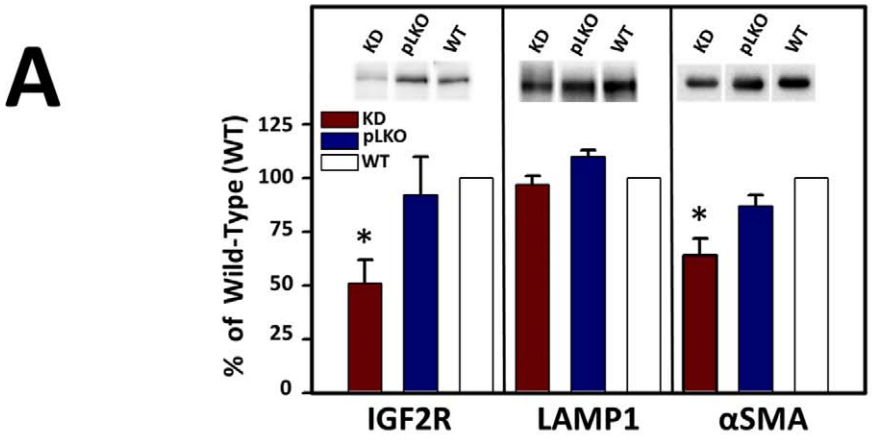

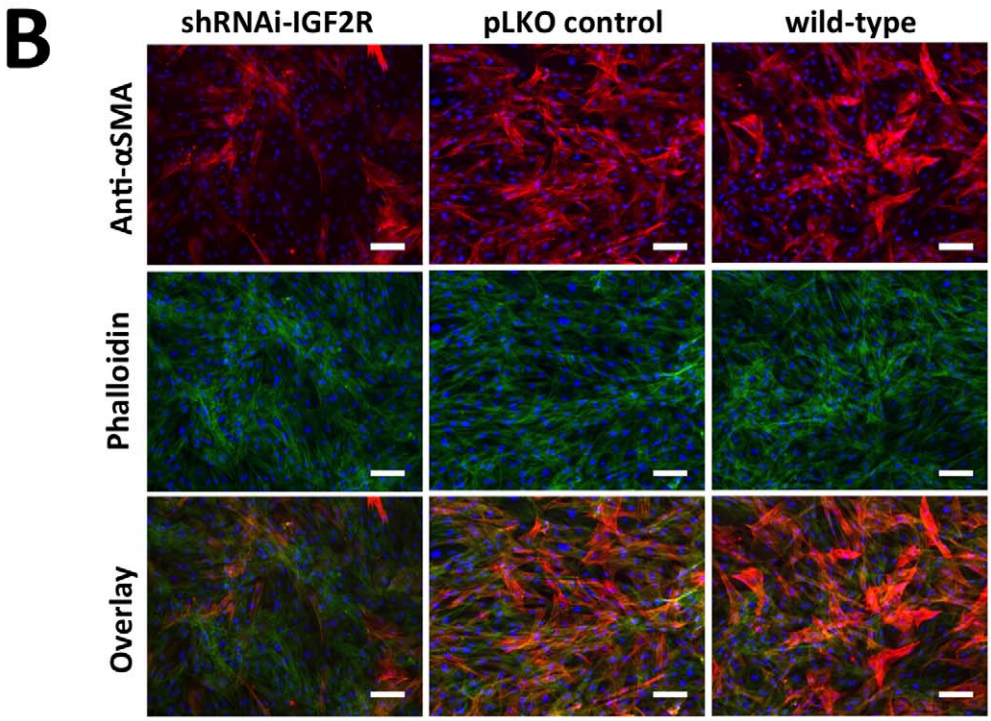

C

% Cells with αSMA Fibrils

Donor	shRNAi	pLKO	wild-type
646	18 ± 2 (n=4)	85 ± 2 (n=4)	82 ± 10 (n=4)
580	51 ± 3 (n=8)	79 ± 1 (n=8)	82 ± 5 (n=8)
842	62 ± 3 (n=10)	84 ± 3 (n=4)	88 ± 2 (n=4)
5860	30 ± 3 (n=8)	94 ± 1 (n=7	95 ± 1 (n=5)
Mean	40 ± 10	86 ± 3	87 ± 3

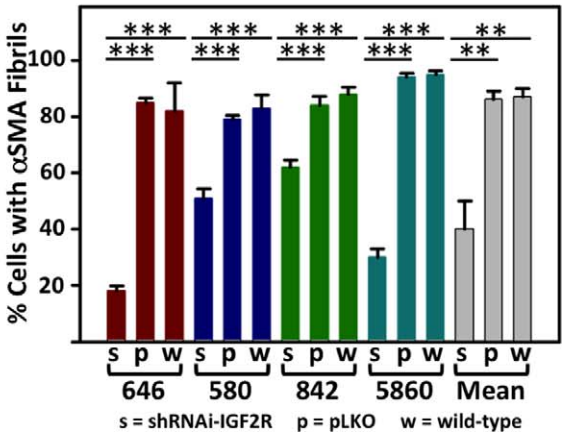

Figure 6. α-SMA fibril formation in primary human corneal myofibroblasts following transduction with control (pLKO) or shRNA-IGF2R lentiviral particles (KD). Lentiviral particle transduced or nontransduced cells (WT) were cultured in 1 ng/mL TGF-β1 for 7 days under serum-free conditions. (**A**) Lysates were generated and subjected to Western blot analysis (equivalent cell numbers loaded into each lane). Membranes were probed with IGF2R-, α-SMA-, or LAMP1-specific antibodies. Quantification is shown below the representative blots and is derived from corneal cultures obtained from four independent donors. Data are plotted as a percentage of the intensity of IGF2R, α-SMA, or LAMP1 bands in the shRNAi-IGF2R KD cells and cells transduced with pLKO control vector relative to nontransduced WT cells set to 100%. Values represent the mean ± SE. The Student's *t*-test was

used to compare the IGF2R KD cells to the pLKO control cells. $^{*}P < 0.02$, $n = 4$. (**B**) Fixed cells were incubated with antibody specific to α-SMA that was visualized using a goat anti-mouse secondary antibody conjugated to Alexa Fluor 568 (*red*) and FITC-conjugated phalloidin (*green*). Nuclei were stained with Hoescht 33342 dye. An overlay of the phalloidin and α-SMA–stained cells is shown in the *bottom*. Representative micrographs are shown. *Scale bar*: 100 μm. (**C**) The images from the studies shown in (**D**) were quantified for the number of cells containing α-SMA fibrils. Approximately 200 to 500 cells per micrograph were scored for the presence of α-SMA–containing fibrils. The percentages shown are derived from four independent donors and are the average for the indicated number (n) of individual micrographs. The mean of the data derived from the four independent human donors also is shown. Values represent the mean ± SE. ANOVA, $P < 0.001$, individual comparisons use the Holm-Sidak method, $^{**}P = 0.002$, $^{***}P < 0.001$.

containing glycan, was added to the fibroblasts, bypassing the activation step of latent TGF-β1. One possible mechanism involves binding of uPAR to domain 1 of IGF2R. uPAR is a glycosylphosphatidylinositol (GPI)-anchored receptor composed of three domains and is involved in modulating extracellular proteolysis, cell adhesion, migration, and signaling.[55,56] Bernstein et al.[57] showed that conversion of corneal fibroblasts to myofibroblasts requires cleavage of the linker region of uPAR between domains 1 and 2, and reduced levels of surface bound uPAR.[57] The IGF2R may facilitate uPAR cleavage by serving as a scaffold for orienting bound uPAR for cleavage by lysosomal proteases or plasmin also bound to IGF2R. Lysosomal proteases, such as cathepsin G, are known to cleave uPAR and to bind IGF2R through their M6P-containing carbohydrate complexes to domains 3, 5, and 9 of IGF2R.[57–59] Plasminogen binds to domain 1 of IGF2R and can be activated to plasmin by uPA-bound uPAR.[26,27,60] Plasmin still bound to IGF2R can cleave and inactivate uPAR. Studies by Nykjaer et al.[25] showed that uPAR is targeted by IGF2R to the lysosome for degradation. Thus, based on the requirement of uPAR cleavage for conversion of fibroblasts to myofibroblasts, the known functions of IGF2R and our data presented here, the mechanism for conversion of fibroblasts to myofibroblasts may require the following steps: IGF2R-facilitated uPAR cleavage, removal of cleaved uPAR from the cell surface by endocytosis of IGF2R-cleaved uPAR complex, trafficking of the complex to the lysosome, and degradation of uPAR. Future studies are needed to test this model.

The IGF2R also may be involved in CTGF-induced fibrosis. A recent study provided evidence that IGF2R is a receptor for CTGF.[28] Because the effects of CTGF on abnormal extracellular matrix production are similar to TGF-β, CTGF is implicated in stimulating corneal scar formation.[61] A lack of IGF2R may alter CTGF protein levels, thereby inhibiting myofibroblast formation. In addition, differentiation of rat kidney fibroblasts to myofibroblasts in culture has been shown to require a combination of TGF-β1, CTGF, and IGF2.[62] Thus, IGF2R may have a critical role in orchestrating the appropriate levels of cytokines and growth factors required for corneal homeostasis and the conversion of fibroblasts to myofibroblasts during wound healing.

The data presented here would suggest inhibition of the synthesis of IGF2R would decrease conversion of fibroblasts to myofibroblasts and could be used to control corneal fibrosis; however, this may adversely alter corneal wound healing because of other functions of the receptor. One of the major roles of the receptor is to bind and transport proteins to the lysosome. This property would be important for the control of extracellular proteins that bind IGF2R and are involved in wound healing: IGF2 which regulates cell proliferation,[35] M6P-containing small leucine-rich glycoproteins,[63] including lumican, which is involved in inflammatory and wound healing processes as well as maintaining corneal transparency,[64] and lysosomal enzymes, which if abnormally secreted degrade extracellular proteins. Because of these important functions of IGF2R, a better approach to controlling myofibroblast formation may be the design and use of molecules that specifically target the interaction of IGF2R with ligands involved in the conversion of fibroblasts to myofibroblasts and in the fibrotic process. For example, small molecules could be identified and used to specifically target the uPAR-binding site in domain 1 (Fig. 1), leaving other critical functions of this receptor intact. Given the multifunctional nature of IGF2R, future studies are warranted to investigate the mechanisms by which IGF2R can influence corneal biology and wound healing.

Acknowledgments

The authors thank Deborah Conklyn for technical assistance. Porcine cornea microscopy was performed at the Microscopy Shared Resource Facility at the Icahn School of Medicine at Mount Sinai.

Supported by NIH Grants DK042667 (NMD), EY021152 (SST), Research to Prevent Blindness Foundation (AMB), National Eye Institute vision core Grant EY01931, and an unrestricted grant from the Research to Prevent Blindness Foundation at the Medical College of Wisconsin.

Disclosure: **R.N. Bohnsack**, None; **D.J. Warejcka**, None; **L. Wang**, None; **S.R. Gillespie**, None; **A.M. Bernstein**, None; **S.S. Twining**, None; **N.M. Dahms**, P

References

1. Wilson SE, Mohan RR, Ambrosio R Jr, Hong J, Lee J. The corneal wound healing response: cytokine-mediated interaction of the epithelium, stroma, and inflammatory cells. *Prog Retin Eye Res* 2001;20:625–637.
2. Hassell JR, Birk DE. The molecular basis of corneal transparency. *Exp Eye Res*. 2010;91:326–335.
3. Lakshman N, Kim A, Petroll WM. Characterization of corneal keratocyte morphology and mechanical activity within 3-D collagen matrices. *Exp Eye Res*. 2010;90:350–359.
4. Wilson SE, Netto M, Ambrosio R, Jr. Corneal cells: chatty in development, homeostasis, wound healing, and disease. *Am J Ophthalmol*. 2003;136:530–536.
5. Maguen E, Zorapapel NC, Zieske JD, et al. Extracellular matrix and matrix metalloproteinase changes in human corneas after complicated laser-assisted in situ keratomileusis (LASIK). *Cornea*. 2002;21:95–100.
6. Jester JV, Petroll WM, Barry PA, Cavanagh HD. Expression of alpha-smooth muscle (alpha-SM) actin during corneal stromal wound healing. *Invest Ophthalmol Vis Sci*. 1995;36:809–819.
7. Mohan RR, Hutcheon AE, Choi R, et al. Apoptosis, necrosis, proliferation, and myofibroblast generation in the stroma following LASIK and PRK. *Exp Eye Res*. 2003;76:71–87.
8. Netto MV, Mohan RR, Ambrosio R Jr, Hutcheon AE, Zieske JD, Wilson SE. Wound healing in the cornea: a review of refractive surgery complications and new prospects for therapy. *Cornea*. 2005;24:509–522.
9. Barbosa FL, Chaurasia SS, Cutler A, et al. Corneal myofibroblast generation from bone marrow-derived cells. *Exp Eye Res*. 2010;91:92–96.
10. Desmouliere A, Redard M, Darby I, Gabbiani G. Apoptosis mediates the decrease in cellularity during the transition between granulation tissue and scar. *Am J Path*. 1995;146:56–66.

11. Desmouliere A, Darby IA, Gabbiani G. Normal and pathologic soft tissue remodeling: role of the myofibroblast, with special emphasis on liver and kidney fibrosis. *Lab Invest*. 2003;83: 1689–1707.
12. Gabbiani G. The myofibroblast in wound healing and fibrocontractive diseases. *J Path*. 2003;200:500–503.
13. Tandon A, Tovey JC, Sharma A, Gupta R, Mohan RR. Role of transforming growth factor Beta in corneal function, biology and pathology. *Curr Mol Med*. 2010;10:565–578.
14. Dahms NM, Hancock MK. P-type lectins. *Biochim Biophys Acta*. 2002;1572:317–340.
15. Brown J, Jones EY, Forbes BE. Keeping IGF-II under control: lessons from the IGF-II-IGF2R crystal structure. *Trends Biochem Sci*. 2009;34:612–619.
16. Oka Y, Rozek LM, Czech MP. Direct demonstration of rapid insulin-like growth factor II Receptor internalization and recycling in rat adipocytes. Insulin stimulates 125I-insulin-like growth factor II degradation by modulating the IGF-II receptor recycling process. *J Biol Chem*. 1985;260:9435–9442.
17. Schmidt B, Kiecke-Siemsen C, Waheed A, Braulke T, von Figura K. Localization of the insulin-like growth factor II binding site to amino acids 1508-1566 in repeat 11 of the mannose 6-phosphate/insulin-like growth factor II receptor. *J Biol Chem*. 1995;270:14975–14982.
18. Bergman D, Halje M, Nordin M, Engstrom W. Insulin-like growth factor 2 in development and disease: a mini-review. *Gerontology*. 2013;59:240–249.
19. Wang ZQ, Fung MR, Barlow DP, Wagner EF. Regulation of embryonic growth and lysosomal targeting by the imprinted Igf2/Mpr gene. *Nature*. 1994;372:464–467.
20. Ludwig T, Eggenschwiler J, Fisher P, D'Ercole AJ, Davenport ML, Efstratiadis A. Mouse mutants lacking the type 2 IGF receptor (IGF2R) are rescued from perinatal lethality in Igf2 and Igf1r null backgrounds. *Dev Biol*. 1996;177:517–535.
21. Ludwig T, Ovitt CE, Bauer U, et al. Targeted disruption of the mouse cation-dependent mannose 6-phosphate receptor results in partial missorting of multiple lysosomal enzymes. *EMBO J*. 1993;12:5225–5235.
22. Ludwig T, Munier-Lehmann H, Bauer U, et al. Differential sorting of lysosomal enzymes in mannose 6-phosphate receptor-deficient fibroblasts. *EMBO J*. 1994;13:3430–3437.
23. Marron-Terada PG, Brzycki-Wessell MA, Dahms NM. The two mannose 6-phosphate binding sites of the insulin-like growth factor-II/mannose 6-phosphate receptor display different ligand binding properties. *J Biol Chem*. 1998;273:22358–22366.
24. Schiller HB, Szekeres A, Binder BR, Stockinger H, Leksa V. Mannose 6-phosphate/insulin-like growth factor 2 receptor limits cell invasion by controlling alphaVbeta3 integrin expression and proteolytic processing of urokinase-type plasminogen activator receptor. *Mol Biol Cell*. 2009;20:745–756.
25. Nykjaer A, Christensen EI, Vorum H, et al. Mannose 6-phosphate/insulin-like growth factor-II receptor targets the urokinase receptor to lysosomes via a novel binding interaction. *J Cell Biol*. 1998;141:815–828.
26. Leksa V, Godar S, Cebecauer M, et al. The N terminus of mannose 6-phosphate/insulin-like growth factor 2 receptor in regulation of fibrinolysis and cell migration. *J Biol Chem*. 2002;277:40575–40582.
27. Bohnsack RN, Patel M, Olson LJ, Twining SS, Dahms NM. Residues essential for plasminogen binding by the cation-independent mannose 6-phosphate receptor. *Biochemistry*. 2010;49:635–644.
28. Blalock TD, Gibson DJ, Duncan MR, Tuli SS, Grotendorst GR, Schultz GS. A connective tissue growth factor signaling receptor in corneal fibroblasts. *Invest Ophthalmol Vis Sci*. 2012;53:3387–3394.
29. Kang JX, Li Y, Leaf A. Mannose-6-phosphate/insulin-like growth factor-II receptor is a receptor for retinoic acid. *Proc Natl Acad Sci U S A*. 1997;94:13671–13676.
30. Wood RJ, Hulett MD. Cell surface-expressed cation-independent mannose 6-phosphate receptor (CD222) binds enzymatically active heparanase independently of mannose 6-phosphate to promote extracellular matrix degradation. *J Biol Chem*. 2008;283:4165–4176.
31. Matzner U, von Figura K, Pohlmann R. Expression of the two mannose 6-phosphate receptors is spatially and temporally different during mouse embryogenesis. *Development*. 1992; 114:965–972.
32. Funk B, Kessler U, Eisenmenger W, Hansmann A, Kolb HJ, Kiess W. Expression of the insulin-like growth factor-II/mannose-6-phosphate receptor in multiple human tissues during fetal life and early infancy. *J Clin Endocr Metab*. 1992;75:424–431.
33. Varela JC, Goldstein MH, Baker HV, Schultz GS. Microarray analysis of gene expression patterns during healing of rat corneas after excimer laser photorefractive keratectomy. *Invest Ophthalmol Vis Sci*. 2002;43:1772–1782.
34. Arnold DR, Moshayedi P, Schoen TJ, Jones BE, Chader GJ, Waldbillig RJ. Distribution of IGF-I and -II, IGF binding proteins (IGFBPs) and IGFBP mRNA in ocular fluids and tissues: potential sites of synthesis of IGFBPs in aqueous and vitreous. *Exp Eye Res*. 1993;56:555–565.
35. Musselmann K, Kane BP, Alexandrou B, Hassell JR. IGF-II is present in bovine corneal stroma and activates keratocytes to proliferate in vitro. *Exp Eye Res*. 2008;86:506–511.
36. Bradford MM. A rapid and sensitive method for the quantitation of microgram quantities of protein utilizing the principle of protein-dye binding. *Anal Biochem*. 1976;72:248–254.
37. Taylor JL, Casey MS, O'Brien WJ. Synergistic antiherpes virus activity of acyclovir and interferon in human corneal stromal cells. *Invest Ophthalmol Vis Sci*. 1989;30:365–370.
38. Jester JV, Barry-Lane PA, Cavanagh HD, Petroll WM. Induction of alpha-smooth muscle actin expression and myofibroblast transformation in cultured corneal keratocytes. *Cornea*. 1996; 15:505–516.
39. Wick DA, Seetharam B, Dahms NM. Basolateral sorting signal of the 300-kDa mannose 6-phosphate receptor. *Am J Physiol Gastrointest Liver Physiol*. 2002;282:G51–G60.
40. Yang Y, Wang Z, Yang H, et al. TRPV1 potentiates TGFbeta-induction of corneal myofibroblast development through an oxidative stress-mediated p38-SMAD2 signaling loop. *PLoS One*. 2013;8:e77300.
41. El-Shewy HM, Lee MH, Obeid LM, Jaffa AA, Luttrell LM. The insulin-like growth factor type 1 and insulin-like growth factor type 2/mannose-6-phosphate receptors independently regulate ERK1/2 activity in HEK293 cells. *J Biol Chem*. 2007;282: 26150–26157.
42. Hinz B, Celetta G, Tomasek JJ, Gabbiani G, Chaponnier C. Alpha-smooth muscle actin expression upregulates fibroblast contractile activity. *Mol Biol Cell*. 2001;12:2730–2741.
43. Hinz B, Gabbiani G. Mechanisms of force generation and transmission by myofibroblasts. *Curr Opin Biotechnol*. 2003; 14:538–546.
44. Tomasek JJ, Gabbiani G, Hinz B, Chaponnier C, Brown RA. Myofibroblasts and mechano-regulation of connective tissue remodelling. *Nat Rev Mol Cell Biol*. 2002;3:349–363.
45. Blanco-Mezquita JT, Hutcheon AE, Zieske JD. Role of thrombospondin-1 in repair of penetrating corneal wounds. *Invest Ophthalmol Vis Sci*. 2013;54:6262–6268.
46. Chandler HL, Colitz CM, Lu P, Saville WJ, Kusewitt DF. The role of the slug transcription factor in cell migration during corneal re-epithelialization in the dog. *Exp Eye Res*. 2007;84:400–411.
47. Rohrer J, Schweizer A, Russell D, Kornfeld S. The targeting of Lamp1 to lysosomes is dependent on the spacing of its

Investigative Ophthalmology & Visual Science

cytoplasmic tail tyrosine sorting motif relative to the membrane. *J Cell Biol*. 1996;132:565–576.

48. Saftig P, Klumperman J. Lysosome biogenesis and lysosomal membrane proteins: trafficking meets function. *Nat Rev Mol Cell Biol*. 2009;10:623–635.
49. Wang X, Appukuttan B, Ott S, et al. Efficient and sustained transgene expression in human corneal cells mediated by a lentiviral vector. *Gene Ther*. 2000;7:196–200.
50. Koh SW, Chandrasekara K, Abbondandolo CJ, Coll TJ, Rutzen ARVIP. and VIP gene silencing modulation of differentiation marker N-cadherin and cell shape of corneal endothelium in human corneas ex vivo. *Invest Ophthalmol Vis Sci*. 2008;49:3491–3498.
51. Weiner JA, Chen A, Davis BH. E-box-binding repressor is down-regulated in hepatic stellate cells during up-regulation of mannose 6-phosphate/insulin-like growth factor- II receptor expression in early hepatic fibrogenesis. *J Biol Chem*. 1998;273:15913–15919.
52. Hao CF, Li XF, Yao W. Role of insulin-like growth factor II receptor in transdifferentiation of free silica-induced primary rat lung fibroblasts. *Biomed Environ Sci*. 2013;26:979–985.
53. Dennis PA, Rifkin DB. Cellular activation of latent transforming growth factor beta requires binding to the cation-independent mannose 6-phosphate/insulin-like growth factor type II receptor. *Proc Natl Acad Sci U S A*. 1991;88:580–584.
54. Godar S, Horejsi V, Weidle UH, Binder BR, Hansmann C, Stockinger H. M6P/IGFII-receptor complexes urokinase receptor and plasminogen for activation of transforming growth factor-beta1. *Eur J Immunol*. 1999;29:1004–1013.
55. Blasi F, Carmeliet P. uPAR: a versatile signalling orchestrator. *Nat Rev Mol Cell Biol*. 2002;3:932–943.
56. Binder BR, Mihaly J, Prager GW. uPAR-uPA-PAI-1 interactions and signaling: a vascular biologist's view. *Thromb Haemost*. 2007;97:336–342.
57. Bernstein AM, Twining SS, Warejcka DJ, Tall E, Masur SK. Urokinase receptor cleavage: a crucial step in fibroblast-to-myofibroblast differentiation. *Mol Biol Cell*. 2007;18:2716–2727.
58. Montuori N, Carriero MV, Salzano S, Rossi G, Ragno P. The cleavage of the urokinase receptor regulates its multiple functions. *J Biol Chem*. 2002;277:46932–46939.
59. Dahms NM, Olson LJ, Kim JJ. Strategies for carbohydrate recognition by the mannose 6-phosphate receptors. *Glycobiology*. 2008;18:664–678.
60. Leksa V, Pfisterer K, Ondrovicova G, et al. Dissecting mannose 6-phosphate-insulin-like growth factor 2 receptor complexes that control activation and uptake of plasminogen in cells. *J Biol Chem*. 2012;287:22450–22462.
61. Wunderlich K, Senn BC, Reiser P, Pech M, Flammer J, Meyer P. Connective tissue growth factor in retrocorneal membranes and corneal scars. *Ophthalmologica*. 2000;214:341–346.
62. Grotendorst GR, Rahmanie H, Duncan MR. Combinatorial signaling pathways determine fibroblast proliferation and myofibroblast differentiation. *FASEB J*. 2004;18:469–479.
63. Sleat DE, Sun P, Wiseman JA, et al. Extending the mannose 6-phosphate glycoproteome by high resolution/accuracy mass spectrometry analysis of control and acid phosphatase 5-deficient mice. *Mol Cell Prot*. 2013;12:1806–1817.
64. Amjadi S, Mai K, McCluskey P, Wakefield D. The Role of lumican in ocular disease. *ISRN Ophthalmol*. 2013;2013:632302.